Bollettino di Geofisica Teorica ed Applicata Vol. 57, n. 1, pp. 31-42; March 2016
DOI 10.4430/bgta0172

Hyperspectral images to monitor oil spills in the River Po

C. Pietrapertosa[1], A. Spisni[2], V. Pancioli[3], A. Pavan[4], P. Sterzai[4], P. Paganini[4], M. Vellico[4], A. Monni[3] and F. Coren[4]

[1] *CNR-IMAA, Istituto di Metodologie per l'Analisi Ambientale, Tito-Scalo (PZ), Italy*
[2] *Servizio Idro-Meteo-Clima, ARPA Emilia-Romagna, Bologna, Italy*
[3] *Agenzia Regionale di Protezione Civile, Regione Emilia Romagna, Bologna, Italy*
[4] *Istituto Nazionale di Oceanografia e di Geofisica Sperimentale (OGS), Trieste, Italy*

(Received: June 24, 2015; accepted: January 26, 2016)

ABSTRACT Knowledge of an oil spill's extent and its quantification are fundamental to limit damage and assess impacts. Remote sensing permits the observation of large areas in a short time, to locate and quantify the phenomenon. We present the case study of the River Lambro, where an oil spill occurred on February 23, 2010 and then flowed into the River Po. The Agenzia di Protezione Civile della Regione Emilia-Romagna quickly commissioned two aerial surveys over the polluted area, performed by Istituto Nazionale di Oceanografia e di Geofisica Sperimentale (OGS) with a hyperspectral sensor, AISA Eagle 1K, in order to obtain qualitative and quantitative assessment of the spilled substances and to support rapid decision-making with real-time monitoring. The method used a Spectral Angle Mapper (SAM) classification to locate the pollution. Results showed a successful applicability in the production of the pollution map used for the containment phase.

Key words: oil spills, remote sensing, hyperspectral imagery, Spectral Angle Mapper (SAM), oil thickness, Rapid Response Systems.

1. Introduction

The River Lambro's oil spill happened during the night between February 22 and February 23, 2010; it was discharged from Lombarda Petroli oil storage facility in Villasanta (Monza, Italy). It reached the River Po on February 24, 2010. The estimated quantity of oil spilled was 2,600 tons: 1,800 tons of heating oil and diesel fuel, lighter than water, and 800 tons of fuel oil, heavier than water. About 300 tons were recovered from containment tanks in the Lombarda Petroli yard. Another part of the oil spill reached the sewage treatment plant of BrianzAcque, which retained a quantity of approximately 1,250 tons of material. A quantity of 1,050 tons reached the River Lambro. Thanks to barriers, another 200 tons were collected before the Lambro met the River Po. Along the River Po, containment actions allowed the recovery of 450 tons of material at the dam of Isola Serafini (Po). Unspecified quantities of the remaining 400 tons evaporated or were deposited on the sides of the river (Dipartimento della Protezione Civile, 2010). The damage was very serious for the river ecosystem, requiring urgent remediation and recovery measures. During the emergency phase, Agenzia di Protezione Civile della Regione Emilia-Romagna set up an action plan. Two remote sensing aerial surveys were performed by Istituto Nazionale di

Oceanografia e di Geofisica Sperimentale (OGS), using its own AISA Eagle 1K Airborne Imaging Spectrometer for Applications, to support the measures used to deal with the emergency (Dondi *et al.*, 2010), mapping the oil along the river flow. The flights took place on February 27 and March 2, 2010. The coverage of the images acquired during the first survey follows the River Po flow from its confluence with the River Lambro (Piacenza Province) to the town of Corbola (Rovigo Province); the second survey goes from Corbola to the Po delta. Due to the emergency situation, it was not possible to plan the flights under ideal weather conditions. In this paper we discuss the results obtained, analyzing the February 27 data set, because it was acquired under better conditions.

2. Background

Oil spill detection on water can be quite a difficult task, due to weather conditions, water movements, the extent of the polluted area, and oil spectral response. Oils can be beneath the water surface or emulsified with it.

Most oils quickly spread horizontally on top of the water. This thin surface is called a *slick*. As time passes, the slick becomes thinner, forming a layer called a *sheen,* which reflects rainbow colours. Floating on water, an oil slick spreads rapidly: the heavy part tends to form sediment, the very light portion tends to evaporate in a few days. Depending on the turbulence of the water, the oil's light portion forms droplets that can have a diameter in the range of 5 μm to a few hundred μm (Korotenko *et al.*, 2002). During movement and dispersion of the oil slick, droplets can coalesce, combining this phenomenon with evaporation and degradation; the thickness of the slick can in this way be reduced to a few tens of μm. Natural dispersion of oil is a very complex process: the oil slick breaks in a shower of "oil" droplets that diffuse downwards and that subsequently can float back to the surface to coalesce or remain dispersed in water (Korotenko *et al.*, 2002). The thickness of the oil spill depends on the chemical and physical properties of the pollutant.

Surface tension, specific gravity, and viscosity determine how the oil diffuses into water or into the atmosphere. Low surface tension will spread oil more easily, high specific gravity will form tar balls on the bottom of the water body. Oil with high viscosity will tend to stay in one place (EPA, 1999).

In water environments, oil's natural degradation can occur in many ways, through physical, chemical, and biological processes. The most common are the following:

- weathering: chemical and physical reactions break down oil chains that become heavier than water. These droplets can be dispersed by waves or form thin films;
- evaporation: this occurs when the more volatile substances of oil become vapours and leave the water surface. This is typical of refined products such as kerosene and gasoline, because they contain a high percentage of very toxic and flammable components that usually evaporate in a few hours. The heavier part of the oil may move down to the water column and then be weathered;
- oxidation: this occurs at the edge of the slicks, where oil interacts with water and oxygen to produce water-soluble compounds;
- biodegradation: when bacteria feed on hydrocarbons. This process is strictly dependent on water oxygenation and on the ecosystem. This biodegradation process is rapid and removes

most of the hydrocarbons (Gearing *et al*., 1980). However, about 20-30% of branched alkanes, cycloalkanes, and aromatics may remain for more than one year. The soluble part (mostly aromatics) can be absorbed by underground water (Eganhouse *et al*., 1996);

- emulsification: this process forms a mixture of oil droplets and water. It can be water in oil or oil in water. In the first case, the oil slick is thick and viscous and can remain in the environment for a long time. In the second case, oil disappears from the surface but is still present at the bottom of it, giving the illusion that the issue is resolved.

Aquatic environments have complex interactions between plant and animal species. Damage to the environment has an impact on the food chain up to humans. In open water, fishes may move away from the polluted area and not be hurt, but in coastal areas, in lakes, or in shallow water, oil may have an impact on vegetation, benthic biota, and other animals, such as reptiles, fishes, amphibians, and mammals. Along a river, the oil tends to deposit near riversides and sand banks. It can be trapped by vegetation such as cane thicket or shrubs (EPA, 1999).

Usually oil spills are more common in saltwater bodies or coastal areas (marine environments) where huge tankers are present. In this kind of environment, oil can be seen using active remote sensing as Synthetic Aperture Radar (SAR) data, able to detect the differences in wave motion. The fluvial/lake bodies (freshwater environments) have a different dynamic compared to the marine one; the analysis phase for fluvial/lake bodies is more difficult because of the smaller water extension, the wave motion absence, the continuous water flows, and the different density of water (seawater is denser than the river water because of salt concentration).

Oil spills can also take place on land. This is common in oil fields, refineries, storage facilities, or along pipelines. On the soil surface, the spill appears as a black patch, but it can also penetrate the soil profile.

Pollutant identification and monitoring can be performed by using different remote sensing instruments: ultraviolet, visible and infrared sensors, microwave radiometers, laser fluorosensors, and laser-acoustic thickness sensors (Jha *et al*., 2008). Actually, the laser fluorosensor is the only instrument that can positively detect different types of oil on most backgrounds, but it has the disadvantage of a large size, and high weight and cost. For these reasons, it is usually less likely to be purchased (Fingas and Brown, 2000). Meanwhile, hand laser-acoustic instruments are being developed because this is the only technology able to measure absolute oil thickness (Fingas and Brown, 2000).

Airborne oil tracking remains the most common method (Fingas and Brown, 2000) for studying oil spill evolution. The Bonn Agreement established in northern European countries tries to define a crisis protocol in case of an oil spill. It sets the guidelines for aerial surveillance (Bonn Agreement, 2007).

In the visible spectrum, oil has a higher response than water, but also has no distinctive features (Brown *et al*., 1996). Sheen appears as a bright surface, reflecting light over a wide spectral region.

False alarms can be detected due to sun glint, wind sheen, and biogenic material such as weeds. Even with those limitations, visible cameras are widely used to monitor and track oil spills because they are cheaper than other instruments.

The hyperspectral passive technique furnishes detailed spectral/spatial signatures for different materials, thanks to the combination of high spatial and spectral resolutions (Salem *et al*., 2005). This can be very useful for Geographical Information Systems (GISs) where technicians may monitor the evolution of the disaster phenomena.

Remote sensing data can be processed in different ways, such as multispectral classification supported by *in situ* data to calibrate oil thickness (Svejkovsky *et al.*, 2012), or computation of ratios and results related to laboratory tests on oil thickness (Lennon *et al.*, 2003). Remote sensing acquisitions should, in fact, be supported by ground spectroscopic measurements of the slick from on board a boat (Lennon *et al.*, 2006). This approach could be possible in experimental sites, but when a rapid response is needed it could be difficult to perform, especially when the spill is not wide and is confined along a river, in which case most of the efforts are dedicated to oil removal.

The goal of these procedures is to identify the oil spill and to provide information about the location and extent of the pollution phenomenon, in order to plan subsequent operations. Since the operational target was to define a picture of the pollution spread across the river flow, it was crucial to adopt a methodology that did not require a time-consuming procedure. The remote sensing acquisitions had to provide information in time to ensure the effectiveness of containment measures.

Under these conditions, the choice was to adopt a methodology based on multispectral classification applied to radiance data, following the approach of Filizzola *et al.* (2002); this methodology maps surface materials using hyperspectral radiance on airborne sensor images and considers a limited set of field observations. No atmospheric, topographic, or illumination corrections were performed on the data.

3. Data acquisition

Data were acquired by a hyperspectral sensor mounted on a Beechcraft Sundowner C23 aircraft. The hyperspectral system Airborne Imaging Spectrometer (AISA) Eagle 1K (developed by Spectral Imaging Ltd, Specim, Finland) is composed of a push-broom sensor able to collect up to 244 bands in the Visible Near Infrared (VNIR) spectrum, a data-acquisition unit in a PC, a GPS receiver, and an inertial navigation system.

The acquisition was performed on February 27, 2010, the average flight altitude was 1,500 m above ground level, swath width was 1 km and the pixel resolution was 1 m; 16 data strips were collected, starting at 11:00 and finishing at 15:08 GMT. Twenty-four hyperspectral bands were acquired for every strip, in the continuous VNIR spectral range, from 400 to 970 nm, with an average bandwidth of 24. The acquired hyperspectral data set was corrected to spectral radiance values ($mW/cm^2 \cdot sr \cdot nm$) and geo-referenced using the Hyper-Spectral Processor (HSP) software package, developed by OGS. The amount of acquired and processed raw data was 15 Gb.

A digital camera (Canon EOS 1Ds Mark III), adapted for aerial acquisitions, was then used to obtain orthophotos. It was connected to the GPS navigation system, in order to get the shutter time and the attitude of the aircraft, for each single frame acquired. 928 photographical frames were acquired simultaneously with the hyperspectral data, with a ground resolution of 0.20 m per pixel. These data were mainly used to assist visual interpretation of phenomena.

During the flight, the head of the spill reached Pontelagoscuro (FE), while a huge slick was still present, just beyond Piacenza and near San Nazzaro (PC). The Po had a river flow of 1370 m^3/s at Piacenza and 1870 m^3/s at Pontelagoscuro. The river flow velocity was approximately 5-6 km/h.

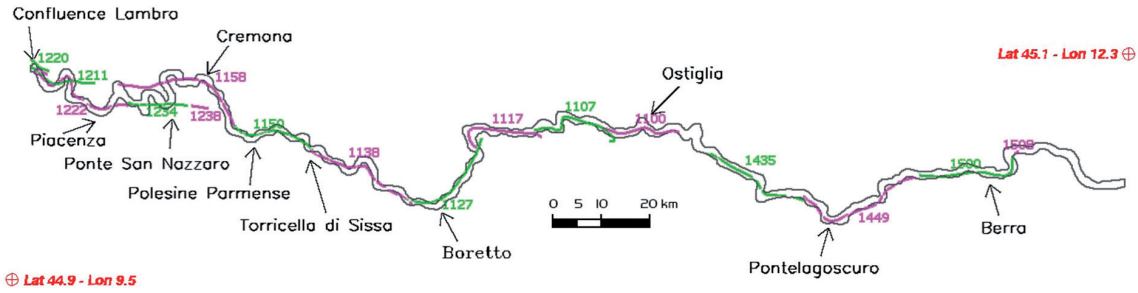

Fig. 1 - February 27, 2010 flight path: black corresponds to the river, magenta and green to the flight path.

Fig. 1 shows the flight path of the acquisition on February 27.

The phenomenon was also monitored through a series of *in situ* measurements along the course of the River Po and the River Lambro. On February 27, some chemical measurements were done, the samples gathered at the water surface, at -1, and -2 m. Table 1 shows the presence of hydrocarbons in the water; samples were collected in three locations from west to east, at Polesine Parmense (PR), Torricella di Sissa (PR) and Boretto (RE). No measurements of oil slick thickness were done. Unfortunately, the samples were collected mainly for drinking water analysis, so they could be used only as a reference for the presence of the pollutants. An ideal sampling method useful for remote sensing analysis should have measured the surface quantity of oil and estimated the thickness. At the same time, since the river flowed at the speed of 5 km/h, the field survey should have taken place at the time of the passage of the plane. These conditions were not viable due to the ongoing emergency measures that were focused primarily on oil containment, oil removal, and citizen safety.

Table 1 - River Po water samples collected during the February 27 field study.

TIME	LOCATION	DEPTH	DISSOLVED HC (mg/L)	TOTAL HC (mg/L)
7.00	Boretto - Pontile Giudecca	0 m	7.80	11.5
7.00	Boretto - Pontile Giudecca	- 1 m	0.06	0.1
7.00	Boretto - Pontile Giudecca	- 2 m	0.07	0.11
9.10	Polesine P.se - pontile attracco	0 m	0.29	0.63
9.10	Polesine P.se - pontile attracco	- 2 m	0.10	0.35
9.50	Torricella di Sissa - pontile attracco	0 m	0.11	0.49
9.50	Torricella di Sissa - pontile attracco	- 2 m	0.03	0.03
10.30	Torricella di Sissa - pontile attracco	0 m	0.15	0.52
13.30	Boretto - Pontile Giudecca	0 m	2.7	4.8
13.30	Boretto - Pontile Giudecca	- 1 m	0.08	0.15

4. Classification: methodology and results

To map the oil on the river surface using hyperspectral data, it is necessary to compare the spectral signature between acquired data and laboratory data or between acquired data and ground-based measurements. This procedure requires data that is corrected for atmospheric interference, illumination, and topographic effects. Typically, the traditional radiometric methods are based on

standard atmospheric models or on the ground-based measurements of atmospheric parameters, but frequently difficulties arise in comparing the spectral reflectance signature measured in the laboratory to the one measured by the sensor, because of the different atmospheric and ancillary conditions.

In this study, the images are corrected for radiance at sensor; no atmospheric correction is performed according to the approach proposed by Filizzola *et al*. (2002). This approach is based on the following requirement: to have samples of the material of interest uniquely identified independent of different illumination conditions in the acquired data set.

The first step is to collect the oil spectral signatures on the differently acquired images, in order to build a spectral library. This was a hard task, because the survey was performed in an emergency situation, so we had only one image where field data were collected less than two hours before the flight time (location Torricella di Sissa, Parma) and these data were not collected at the surface. In order to collect a higher number of spectral signatures in different conditions, we examined all the acquired images and identified oil on the water using the known properties of oil and the appearance and colour of oil as suggested by the Bonn Agreement (2009).

Svejkovsky and Muskat (2006) report the difficulties of thickness measurements *in situ*. In their study, they measure thickness first in a special pool subdivided in plots with various sample thicknesses. In the same study they also report the comparison between appearance and thickness.

Oil is affected by the fluorescence phenomenon: it absorbs electromagnetic radiation at wavelengths < 400 nm and emits in the range between 400 and 650 nm (Lennon *et al*., 2003). As a net effect, an optical contrast between oil and the surrounding water appears (Fig. 2). The enhancements of different colour bands pointed out the presence of oil on the river. Detailed analysis of images pointed out macroscopic phenomena in two of them, one acquired near the River Lambro, and another one acquired near the bridge of San Nazzaro, where skimmers and floating barriers were present. The simultaneous recognition of these phenomena in the hyperspectral data and orthophotos helped delineate a set of regions of interest.

Fig. 2 reports an orthophoto on the left side and an AISA image in false colour (red: 801 nm, green: 670 nm, blue: 552 nm) on the right; the orthophoto and the hyperspectral image were

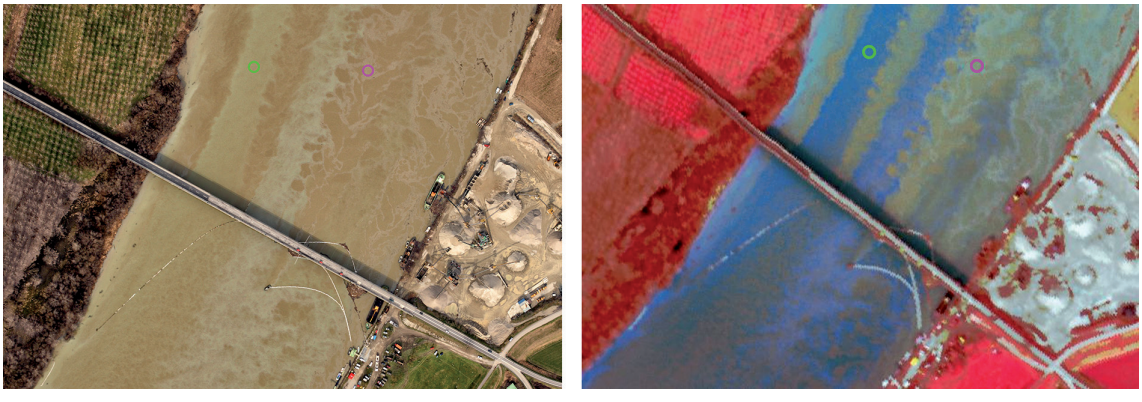

Fig. 2 - San Nazzaro near Piacenza (12:34 GMT). On the left: the orthophoto in real colours shows unpolluted water with a green circle, while the magenta circle indicates oil. On the right: corresponding AISA radiance image in false colours.

acquired simultaneously on the San Nazzaro bridge, where the spectral signatures were acquired. In both images, the green circle indicates the river water, while the magenta circle indicates the oil on the water: a strong reflectance of water at blue and green wavelengths is evident.

In the range of the visible spectrum, from 400 to 700 nm, oil slick appearance depends on different factors: weather, oil concentration, altitude, and meteorological conditions. A contrast enhancement of false colours was applied to the image and underlined the differences among the detected areas. Based on the visual colour image interpretation and known oil textures, we identified five situations or classes for the superficial state of the river in the previous images:

- water: it has to be distinguished between clear water and turbid water;
- film: the water assumes the colour brownish iridescent or brownish sheen;
- concentrate: the colour is brownish concentrate;
- aggregate: brownish aggregate or dark aggregate;
- deposit: heterogeneous suspension (hydrocarbons and brushwood).

According to the Bonn Agreement (2009), oil appearance on the acquired images changes from dark-brown to silver-grey sheen with respect to slick thickness. In Table 2, we report the five categories of the Bonn Agreement Oil Appearance Code (BAOAC); these categories describe the relationship between the appearance of oil on the sea surface and the thickness of the oil layer (Bonn Agreement, 2009).

Table 2 - Bonn Agreement oil appearance code.

Code	Description appearance	Layer thickness interval (μm)	Litres per km^2
1	Sheen (silver/green)	0.040 to 0.30	40 - 300
2	rainbow	0.3 to 5.0	300 - 5000
3	metallic	5 to 50	5000 – 50.000
4	Discontinuous true oil colour	50 to 200	50.000 – 200.000
5	Continuous true oil colour	More than 200	More than 200.000

The regions of interest (Rois) used were defined in the images where pollution was visually evident, especially in the area of Isola Serafini and the bridge of San Nazzaro, near Piacenza. The area was covered by flight strips at 12:22 and 12:34 GMT approximately, during the acquisition.

The Rois statistics are represented by an average of more than one polygon. Some Rois were selected as a reference, like vegetation, to prevent misclassification. We identified 5 classes reported in Table 3.

Table 3 - Classes identification.

Classes	Polygons	Pixel
Water	15	1,673
Film	15	1,125
Concentrate	31	3,270
Aggregate	11	236
Vegetation	3	32,040

The Rois were processed to generate spectral signatures applied to the whole data set. The spectral radiance signatures acquired by AISA (except for vegetation) are displayed in Fig. 3. They are plotted in the range from 412 to 696 nm. The high value assumed by the film class in the range from 500 to 670 nm indicates that the oil sheen has a reflection higher than other classes; the film reflection tends to coincide with clear water for wavelengths close to 696 nm. To prevent the misclassification of classes 1 and 2 (Table 2), they were aggregated, since it was difficult to distinguish between them.

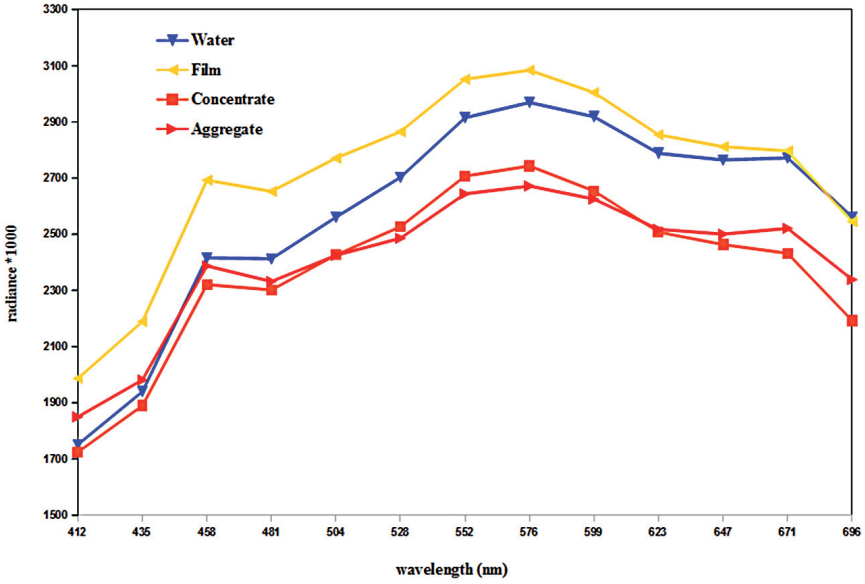

Fig. 3 - Oil spill classes vs. water (in the range 412 - 696 nm).

The geocoded images were classified on the basis of the foregoing identified classes using the Spectral Angle Mapper (SAM) technique (Kruse *et al.*, 1993), included in the ENVI software package (EXELIS Visual Information Solutions). The SAM classification algorithm was applied, because it is not influenced by solar illumination and accentuates the spectral characteristics, supporting Filizzola *et al.* (2002) approach and preventing issues regarding the time of acquisition during the flight. The similarity between pixel spectral radiance signature and the identified targets was found selecting pure pixels in any class during the classification phase. A mask was applied to every image in order to eliminate the ground pixels corresponding to ambiguities, such as riversides, isles, piers and other manmade structures. A deposit class was not considered in the analysis because of the presence of a lot of spurious pixels (sand, shadows, foliage, trunks, etc.).

The initial results prove that the method is efficient for distinguishing clear water from polluted water. It is interesting to note that the harbour area and a second branch not touched by the stream are classified as pure water (see Fig. 4). These results are comparable to *in situ* measurements presented in Table 1; the samples taken in the same area at different times confirm the presence of hydrocarbons. In the Torricelle di Sissa area, the classification shows diffuse oil as concentrate and film flowing along the river's main stream.

The whole classification is represented in Fig. 5, where pollution and its extension are highlighted. The correspondent values are summarized in Table 4.

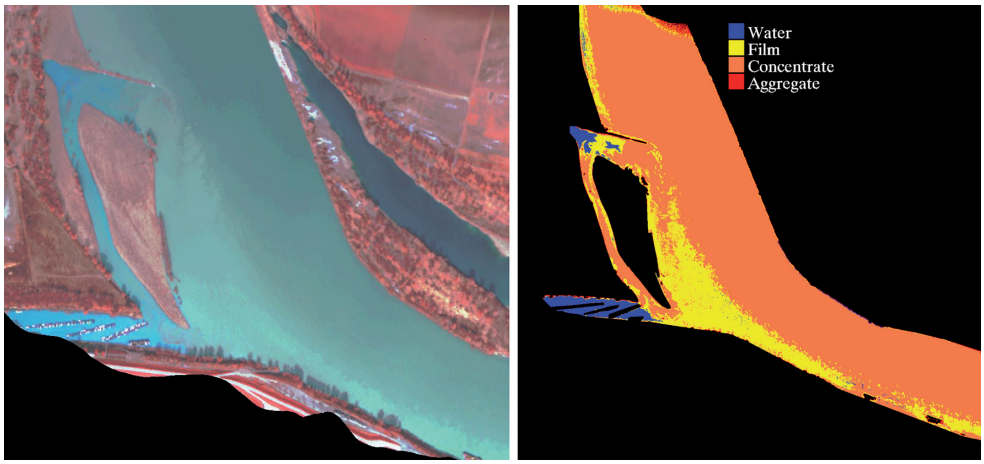

Fig. 4 - Torricella di Sissa: on the left the true colour AISA image, on the right its classification.

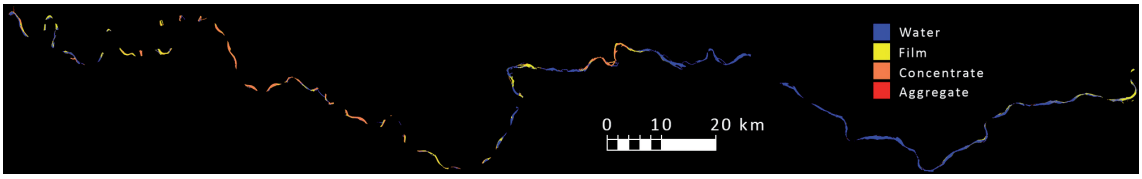

Fig. 5 - Classification map.

Table 4 - Water and pollution extension estimation.

Classes	km² extension	% extension
Water	31	55%
Film	12	22%
Concentrate	12	22%
Aggregate	0.6	1%

The percentage of pollutant extension in the image permitted the identification of oil distribution and features at that time. As shown in Fig. 6, we can divide the map into three macro areas according to the pollutant distribution: Sector 1, Sector 2, and Sector 3. Sector 1 is characterized by the greatest pollution extension percentage. The percentage has been calculated according to the overall surveyed river area.

5. Quantitative analysis estimation

In this study, we made an attempt to estimate the amount of floating oil on water in the geocoded classification map. According to Svejkovsky *et al.* (2012), simultaneous field measurements are difficult to obtain during a real oil spill, and a difficult challenge remains also due to the variability of the water background and illumination. At the same time, the way in which oils interact with water depends on temperature, waves, salinity, and other environmental parameters.

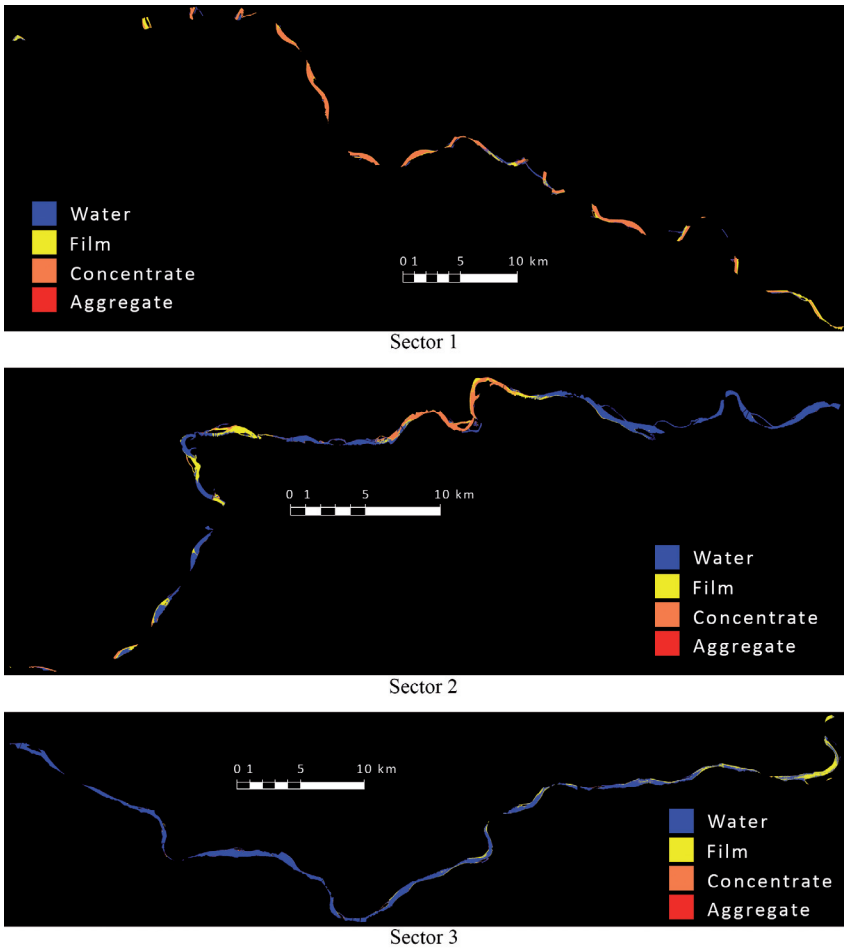

Fig. 6 - Classification map: a) Sector 1, b) Sector 2, c) Sector 3.

In our classification, the appearance of oil varies from brownish sheen to dark. Considering the Bonn Agreement oil appearance code as a reference (Bonn Agreement, 2009), Table 5 relates classes to codes, appearance description, and the average layer thickness used for the oil spill along the river. In accordance with Table 2, we considered an average thickness value for each class of pollutants.

An average density equal to 0.85 t/m³ was fixed for the three different classes: film, concentrate, and aggregate (http://www.safewater.org/PDFS/resourcesknowthefacts/Oil_Spills.pdf). We

Table 5 - BAOAC layer thickness applied to Po case.

Classes	Code (Bonn Agreement)	Description appearance	Average layer thickness interval (μm)
water			
film	1 and 2	Sheen (silver/green) and rainbow	2.5
concentrate	3	metallic	25
aggregate	4	Discontinuous true oil colour	100
deposit		hydrocarbons and brushwood	

calculated the volumes of pollutants for every class, multiplying the average layer thickness of Table 5 by the extension of Table 4 (see Table 6). Finally, thanks to the average density information, we estimated the total pollutant mass present on the water surface; it is about 338 t. This result is coherent with the quantity of pollutant estimated by the Dipartimento della Protezione Civile (2010).

Table 6 - Volume of each class.

Classes	Volume (m^3)
Film	30
Concentrate	309
Aggregate	58

6. Conclusions

The oil spill along the River Po in 2010 was monitored using an AISA hyperspectral sensor and a very high-resolution RGB camera. The AISA images were classified according to a spectral library defined on the acquired data sets. The first oil spill distribution map was delivered three days after the event. Applying the Bonn Agreement oil appearance code to the identified classes, it was possible to identify different oil thicknesses and to approximately estimate the quantity of oil spill in the river at the moment of the aerial survey. The location of oil and its thickness can be helpful to ground operations (containment monitoring systems, positioning of new barriers, etc.) in real time during the first emergency phase.

Some difficulties arose in the analysis phase due to the fluvial environment, in particular the presence of turbid water, central currents, and river bends. Turbidity can affect the colour of the water and therefore the spectral signature detection.

This experience revealed how important it is to set up a local remote sensing protocol to precisely define the planning and all of the related necessary processing steps for a successful aerial survey. From this experience and considering what was suggested by Bajić (2012), we can state that it is necessary to define a protocol for hyperspectral data acquisition in emergency situations focused on the following key issues:

- a detailed airborne flight plan related to the target requiring investigation;
- an accurate selection of the spectral range bands to acquire only the most significant data;
- an estimate of the pre- and post-processing phase time requirement, which is significant when the surveyed area is large and hyperspectral data are to be processed;
- the possibility of performing a simultaneous acquisition of geo-referred data *in situ*, the minimum information possibly being the presence or absence of oil at the surface.

The organization and synergy of these activities constitutes an important added value to environmental protection.

Acknowledgements. Many thanks to A. Spisni (Dept. of Experimental Medicine, University of Parma, Italy) for his support in the definition of oils chemistry and its behaviour in water. Preliminary outcomes were presented in: Pietrapertosa C., Spisni A., Pancioli V., Sterzai P., Pavan A., Paganini P., Monni A. and Coren F. (2010), Utilizzo di immagini iperspettrali per il monitoraggio di sversamento di idrocarburi nel fiume Po, Atti 14ª Conf. Nazionale ASITA, Brescia, Italy, pp. 1457-1462.

REFERENCES

Bajić M.; 2012: *Airborne hyperspectral surveillance of the ship-based oil pollution in Croatian part of the Adriatic sea*. Geod. list, **2**, 77-100.

Bonn Agreement; 2007: *Bonn Agreement aerial surveillance handbook, 2004*. Bonn Agreement Accord de Boon, London, United Kingdom, 37 pp.

Bonn Agreement; 2009: *Bonn Agreement aerial operation handbook 2009, Part 3: Guidelines for oil pollution detection, investigation and post flight analysis/evaluation for volume estimation*. Bonn Agreement Accord de Boon, London, United Kingdom, part 3, Annex A 26 pp.

Brown H.M., Bittner J.P. and Goodman R.H.; 1996: *The limits of visibility of spilled oil sheens*. In: Proc. 2nd Int. Airborne Remote Sens. Conf. Exhibition, San Francisco, CA, USA, vol. III, pp. 327-334.

Dipartimento della Protezione Civile; 2010: *Rapporto attività fiumi Lambro e Po*. Presidenza del Consiglio dei Ministri, Roma, Italy, 12 pp., <http://www.protezionecivile.gov.it/resources/cms/documents/Rapporto_Attivita_Lambro_rev.pdf>.

Dondi C., Lo Jacono F., Sambenedetto G. and Tinti S.; 2010: *Si risolve in Emilia l'emergenza Lambro-Po*. Salvo l'Adriatico, Ecoscienza, **1**, 45-47.

Eganhouse R.P., Dorsey T.F., Phinney C.S. and Westcott A.M.; 1996: *Processes affecting the fate of monoaromatic hydrocarbons in an aquifer contaminated by crude oil*. Environ. Sci. Technol., **30**, 3304-3312.

EPA; 1999: *Understanding oil spills and oil spill response*. EPA 540-K-99-007, U.S. Environ. Protection Agency, Washington, DC, USA, 50 pp.

Filizzola C., Pergola N., Pignatti S. and Tramutoli V.; 2002: *Aerial remote sensing hyperspectral techniques for rocky outcrops mapping*. Ann. Geophys., **45**, 233-245.

Fingas M.V. and Brown C.E.; 2000: *Review of oil spill remote sensing*. In: Proc. 5th Int. Conf. Remote Sens. Marine Coastal Environ., Darwin, Australia, vol. 1, pp. 211-218.

Gearing P.J., Gearing J.N., Pruell R.J., Wadé T.L. and Quinn J.G.; 1980: *Partitioning of No. 2 fuel oil in controlled estuarine ecosystems sediments and suspended particulate matter.* Environ. Sci. Technol., **14**, 1129-1136.

Jha M.N., Levy J.K. and Gao Y.; 2008: *Advances in remote sensing for oil spill disaster management: state-of-the-art sensors technology for oil spill surveillance*. Sens., **8**, 236-255.

Korotenko K.A., Mamedov R.M. and Mooers C.N.K.; 2002: *Prediction of the transport and dispersal of oil in the south Caspian Sea resulting from blowouts*. Environ. Fluid Mech., **1**, 383-414.

Kruse F.A., Lefkoff A.B., Boardman J.W., Heidebrecht K.B., Shapiro A.T., Barhon P.J. and Goetz A.F.H.; 1993: *The Spectral Image Processing System (SIPS) - Interactive visualization and analysis of imaging spectrometer data*. Remote Sens. Environ., **44**, 145-163.

Lennon M., Mariette V., Coat A., Verbeque V., Mouge P., Borstad G.A., Wills P., Kerr R. and Alvarez M.; 2003: *Detection and mapping of the November 2002 prestige tanker oil spill in Galicia, Spain, with the airborne multispectral CASI sensor*. In: Proc. 3rd EARSeL Imaging Spectroscopy Workshop, Herrsching, Germany, 7 pp.

Lennon M., Babichenko S., Thomas N., Mariette V., Mercier G. and Lisin A.; 2006: *Detection and mapping of oil slick in the sea by combined use of hyperspectral imagery and laser-induced fluorescence*. EARSeL eProceedings, **5**, 120-128.

Salem F., Kafatos M., El-Ghazawi T., Gomez R. and Yang R.; 2005: *Hyperspectral image assessment of oil-contaminated wetland*. Int. J. Remote Sens., **26**, 811-821.

Svejkovsky J. and Muskat J.; 2006: *Real-time detection of oil slick thickness patterns with a portable multispectral sensor*. Final report for U.S. Dept. Interior (Minerals Management Service), contract no. 0105CT93144, 37 pp.

Svejkovsky J., Lehr W., Muskat J., Graettinger G. and Mullin J.; 2012: *Operational utilization of aerial multispectral remote sensing during oil spill response: lesson learned during the Deepwater Horizon (MC-252) spill*. Photogramm. Eng. Remote Sens., **78**, 1089-1102.

Corresponding author: Paolo Paganini
Istituto Nazionale di Oceanografia e di Geofisica Sperimentale
Borgo Grotta Gigante 42c, 34010 Sgonico (TS), Italy
Phone: +39 040 2140343; fax: +39 040 327307 e-mail: ppaganini@inogs.it